Korean J. Chem. Eng., 32(3), 373-382 (2015)
DOI: 10.1007/s11814-014-0187-z

pISSN: 0256-1115
eISSN: 1975-7220

Capture of CO_2 from coal using chemical-looping combustion: Process simulation

Ming Luo, Shuzhong Wang†, Jiabin Zhu, Longfei Wang, and Mingming Lv

Key Laboratory of Thermo-Fluid Science and Engineering of MOE, School of Energy and Power Engineering, Xi'an Jiaotong University, Xi'an 710049, P. R. China

(*Received 3 April 2014 • accepted 1 July 2014*)

Abstract−Coal direct chemical-looping combustion (CLC) and coal gasification CLC processes are the two basic approaches for the application of the CLC technology with coal. Two different combined cycles with the overall thermal input of 1,000 MW (LHV) were proposed and simulated, respectively, with $NiO/NiAl_2O_4$ as an oxygen carrier using the ASPEN software. The oxygen carrier circulation ratio in two CLC processes was calculated, and the influence of the CLC process parameters on the system performance such as air reactor temperature and the turbine inlet supplementary firing temperature was investigated. Results found were that the circulation ratio of the oxygen carrier in the coal gasification CLC process is smaller than that in the coal direct CLC process. In the coal direct CLC combined system, the system efficiency is 49.59% with the CO_2 capture efficiency of almost 100%, assuming the air reactor temperature at 1,200 °C and the fuel reactor temperature at 900 °C. As a comparison, the system efficiency of coal gasification CLC combined system is 40.53% with the CO_2 capture efficiency of 85.2% when the turbine inlet temperature is at 1,350 °C. Increasing the supplementary firing rate or decreasing the air reactor temperature can increase the system efficiency, but these will reduce the CO_2 capture efficiency.

Keywords: Chemical-looping Combustion, Coal, CO_2 Capture, ASPEN Plus

INTRODUCTION

With an in-depth understanding of global warming, the reduction of carbon dioxide emission has become the focus of attention around the world. The concentration of CO_2 in the atmosphere today is approximately 398.03 ppm [1], more than 40% higher than the pre-industrial level of 280 ppm [2].

Combustion of fossil fuels releases a massive amount of carbon dioxide into the atmosphere. It is estimated that fossil fuel power generation contributes to about one-third of the total carbon dioxide released from fuel combustion [3].

Several different technologies have been suggested to capture CO_2 in a pure stream from combustion in a fossil fuel power production unit. The three most common technologies are pre-combustion, oxy-fuel combustion and post-combustion [2,4-6]. These techniques are energy-intensive, resulting in a significant decrease of the overall combustion efficiency, and as a result, increase the produced electricity price. Chemical looping combustion (CLC) is a most promising technology to combine fuel combustion and pure CO_2 production in situ, allowing CO_2 sequestration without extra energy supplemented. Thus, CLC is potentially much economic because no costly gas-separation equipment is necessary.

The CLC process using gaseous fuels has been widely investigated, but recently the CLC process using solid fuels has attracted great attention [7]. Because the fuel supply cannot fully support the energy needs of the electricity demand of the country for a long term and solid coal is considerably more abundant than natural gas, it would be highly advantageous if the CLC process could be adapted for solid fuels, especially for China.

There are basically three approaches to the application of CLC technology to solid fuel. The first approach is coal gasification CLC, in which solid fuel is gasified in a separate gasifier with pure oxygen to produce syngas, then the syngas can be used in a CLC unit for gaseous fuel.

In the gasifier, there are pyrolysis reactions, gasification reactions, etc.

First, coal pyrolysis occurs and mainly produces coal char and gases (CO, H_2, CO_2, CH_4, etc.).

$$\text{Coal} \rightarrow \text{coal char+gases (CO, } H_2\text{, } CO_2\text{, } CH_4\text{, etc.)} \quad (1)$$

Simultaneously, char gasification happens. The following main reactions may be considered:

$$C+CO_2 \rightarrow 2CO \quad (2)$$

$$C+H_2O \rightarrow CO+H_2 \quad (3)$$

$$C+O_2 \rightarrow CO_2 \quad (4)$$

$$CO+H_2O \rightarrow CO_2+H_2 \quad (5)$$

Reactions (2) and (3) are endothermic, and can be considered as the most important in a gasification process. O_2 is introduced and the oxidation reaction (4) happens to provide the energy needed for the promotion of reactions (2) and (3). The shift reaction (5) occurs mainly at high steam concentrations.

The raw syngas is then cleaned and introduced into the fuel reactor (FR). In the FR, the oxygen carrier is reduced by the syngas. Here, the oxygen carrier is using NiO/Ni as an example.

$$NiO+H_2=Ni+H_2O \quad (6)$$

†To whom correspondence should be addressed.
E-mail: szwang@aliyun.com
Copyright by The Korean Institute of Chemical Engineers.

$$NiO+CO=Ni+CO_2 \quad (7)$$

Then, Ni is transported to the AR to be oxidized back to NiO.

$$2Ni+O_2=2NiO \quad (8)$$

However, an energy-intensive air separation unit is required for this approach. Therefore, it dramatically increases the cost of the CLC system.

The second approach is the coal direct CLC process, in which the solid fuel is introduced directly to the fuel reactor, where the oxygen carrier is mixed with the fuel directly, giving a one-step fuel oxidation with no need for air separation. However, due to low solid-solid contact efficiency, a solid-solid reaction between the solid fuel and a metal oxide is not likely to occur at an appreciable rate [8,9]. Instead, the solid fuel needs to be gasified and then the oxygen carrier particles react with the gas produced. In the FR, there are also pyrolysis reactions (reaction 1) and gasification reactions (reactions 2-3), etc. Simultaneously, the oxygen carrier is reduced by pyrolysis gases and gasification products (reactions 6-7). A shift reaction (5) also occurs at high steam concentrations. However, in this process, the heat needed for the promotion of reactions (2) and (3) is not supplied by the fuel combustion, but by the transport of oxygen carrier from the AR; thus reaction (4) will not happen. However, the gasification process has been proven to be the time-limiting step [8,10-13].

One more approach for the application of solid fuel in chemical looping process was proposed and investigated by Mattisson et al. [9,14-19]. This process is called chemical looping with oxygen uncoupling (CLOU) method. With this technology, solid fuel is burnt with gas-phase oxygen released from an oxygen carrier in the fuel reactor. But the oxygen carrier for CLOU needs to react reversibly with gas-phase oxygen at high temperature. This approach is not considered in this paper.

The system integration and economic analysis are one of the focus of the CLC process. The system simulations using methane or natural gas have been investigated [20-22]. Results found were that the exergetic power efficiency of CLC-GT system when using Fe_2O_3 as an oxygen carrier is 3.53 percentage points higher than that of the conventional system. Considering the CO_2 inherent separation, the CLC-GT system has greater advantage than theconventional process [20]. Klemens et al. [22] conducted q simulation of q CLC power plant using methane. It was found that the net electric efficiency of such a small scale plant could be expected to be in the range of 32.5-35.8%.

There are also two ways of system integration with CLC process using solid fuels. One is to couple with a fuel gasification process, and another way is direct use of solid fuels. Xiang et al. [23] studied the performance of the combined cycle using ASPEN software. It was found that, assuming an air reactor temperature of 1,200 °C, a gasification temperature of 1,100 °C, and a turbine inlet temperature after supplementary firing of 1,350 °C, the system has the potential to achieve a thermal efficiency of 44.4% (low heating value) with 90.1% of the CO_2 captured. Xiang et al. [24] investigated the performance of a three reactor CLC. In this system, coal is first gasified in a Shell gasifier, following which syngas is introduced to the CLC process for producing hydrogen and electricity. Gnanapragasam et al. [25] and Li et al. [26] also investigated the solid fuel direct chemical looping process to produce hydrogen and/or electricity. Li et al. [26] found that the biomass direct chemical looping process can produce hydrogen and/or electricity at any ratio. When all the oxygen carrier materials were used for power production, the system efficiency was 38.1%. With the CO_2 sequestration, the BDCL becomes a carbon negative process from the life cycle standpoint. Therefore, the process has great potential for clean and efficient biomass utilization.

However, there is also no direct comparison of the basic approaches

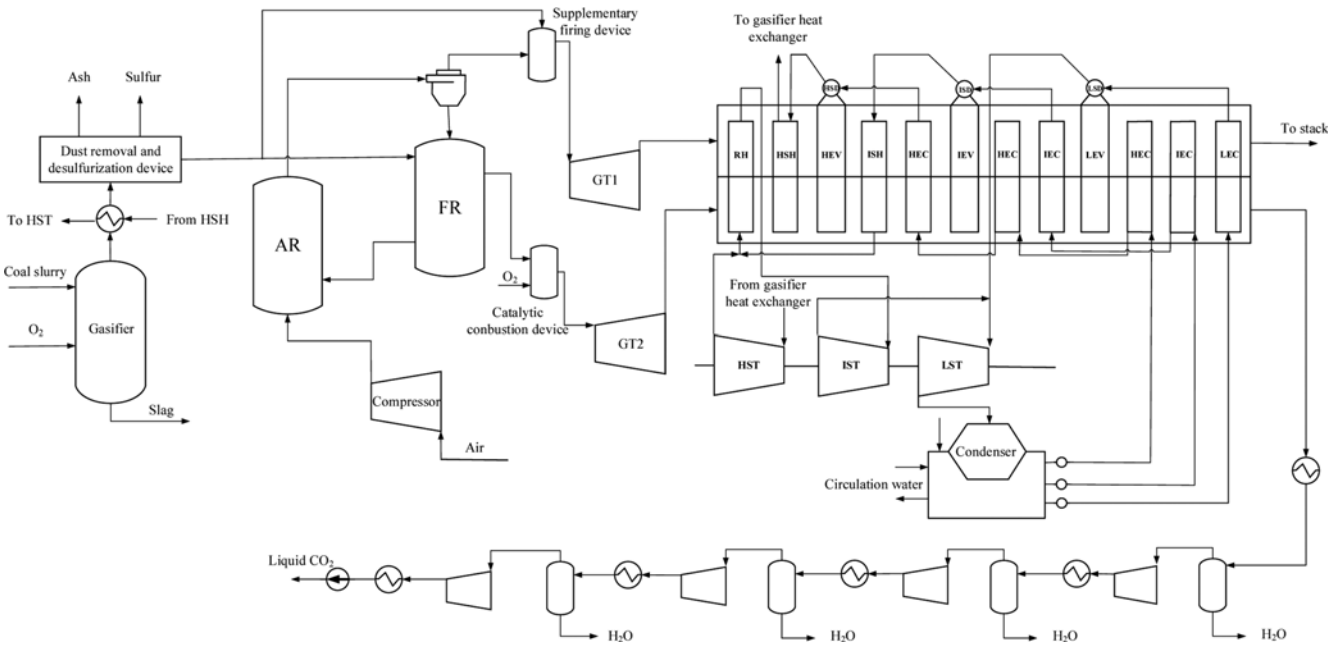

Fig. 1. Schematic diagram of coal gasification CLC combined cycle.

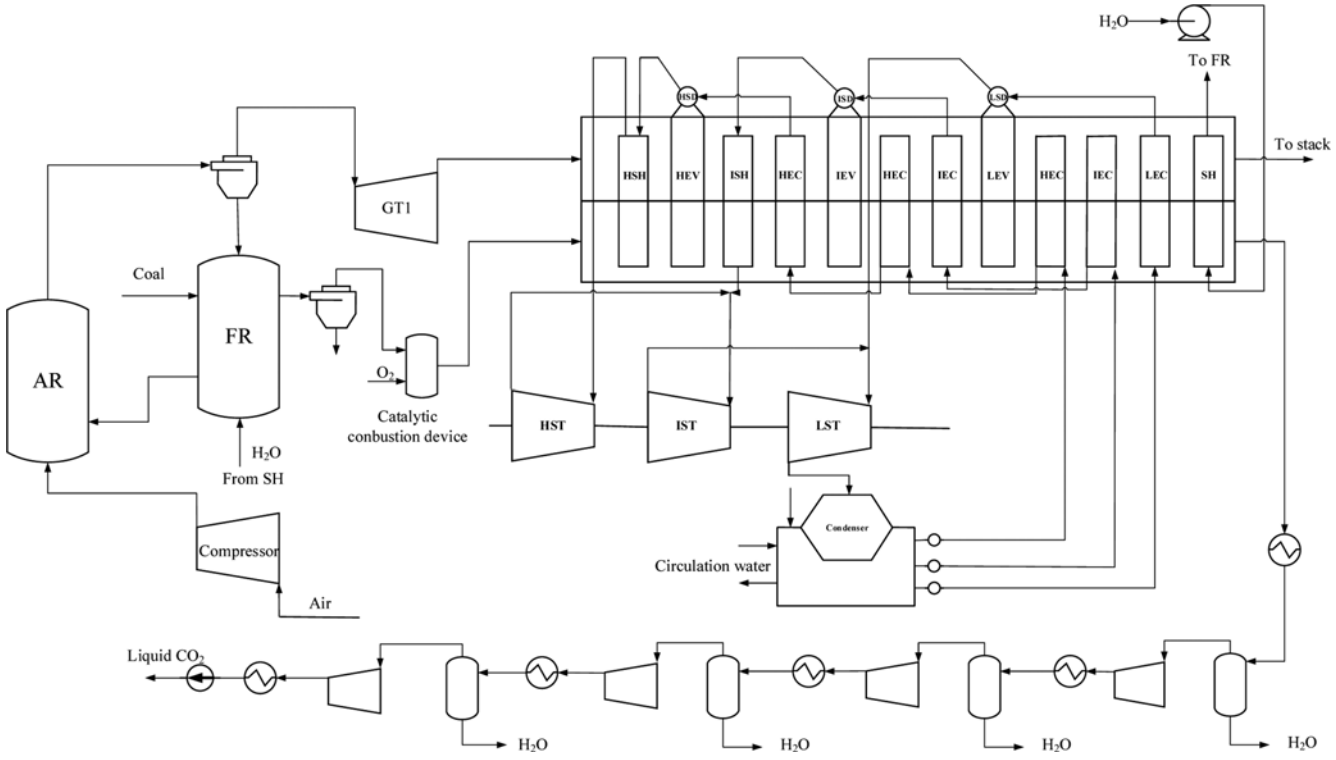

Fig. 2. Schematic diagram of coal direct CLC combined cycle.

to the application of the CLC technology with coal for power generation. Two different combined cycles were proposed and simulated respectively for these two processes using $NiO/NiAl_2O_4$ as an oxygen carrier. The performance of the two combined cycles including the system efficiency and the CO_2 capture efficiency was investigated.

SYSTEM DESCRIPTION

A schematic diagram of the coal gasification CLC combined cycle is shown in Fig. 1. The system is composed of a coal gasifier, CLC reactors, gas turbine, heat recover steam generator (HRSG) and CO_2 compressor. As Texaco entrained flow gasifiers have been widely used throughout the world to produce electric power [27], one is selected in this work. The coal is crushed and mixed with water to produce a slurry and is pumped into the gasifier with oxygen. The raw fuel gas produced is cooled and cleaned through the dust removal and desulfurization device, and then is injected into the fuel reactor (FR), where the oxygen carrier materials are reduced. The heat management and integration is mainly based on the energy cascade utilization principle. The flue gas of the FR (mainly CO_2 and H_2O) drives a gas turbine to generate power. The heat from the gas turbine exhaust is used to generate superheated steam in the HRSG. The hot syngas produced in the Texaco gasifier is cooled initially and radiant heat exchanger is used to recover thermal energy and generate high temperature and pressure steam. Due to the high temperature level, this high temperature waste heat is used to heat the steam from a high pressure superheater (HSH) to the set temperature. The generated superheated steam drives a steam turbine, producing additional power, after which liquid CO_2 can be obtained from the gas exit after cooling, compressing, condensing and water separation. The compressed air is introduced to AR to oxide the reduced oxygen carrier. To increase the system efficiency, the depleted air is introduced to gas turbine after supplementary firing. Then the heat is recovered in the HRSG and the depleted air is finally rejected to stack.

A schematic diagram of the coal direct CLC combined cycle system is shown in Fig. 2. In this system, coal is directly introduced to FR, where the coal pyrolysis and gasification reactions happens. Simultaneously, the oxygen carrier is reduced by pyrolysis and gasification products. The following procedures including the gas turbine power generation, the heat recover, and the CO_2 compress and separation are familiar with that of coal gasification CLC process. However, the gases from FR are introduced into the HRSG but not the gas turbine.

In this paper, ASPEN Plus was employed to investigate the performance of the system. The Texaco gasifier, the AR, and the FR were all simulated by RGIBBS block, where an equilibrium analysis was conducted through the technique of Gibbs free energy minimization. The oxygen was supplied by an ASU, but the ASU is not modeled here. The specific work of 0.4 kWh/kg was adopted during calculation. The key assumptions for performance simulation are shown in Table 1.

1. Gasification Process

Illinois 6# coal was selected and the proximate and ultimate analyses of the coal samples are listed in Table 2. The overall thermal input for the coal direct CLC and coal gasification CLC system are both set at 1,000 MW (LHV). Coal is gasified in the gasifier, and

Table 1. Key assumptions for performance simulation

Progress	Assumption
Gasification process	Temperature, 1,371 °C; pressure, 42.4 bar; carbon conversion rate, 99%; water/coal ratio, 33.5 : 66.5; heat loss, 1% of input LHV
Radiant/convective cooling system	Output temperature of the syngas, 815.6 °C/343.3 °C; Pressure, 41.54 bar
Gas cleaning	Sulfur removal efficiency, 98.5%
Oxygen carrier	$NiO/NiAl_2O_4$ (60 wt% : 40 wt%)
Fuel reactor (FR)	Temperature, 900 °C; thermal loss, 0.5% of thermal input
Air reactor (AR)	Temperature, 950-1,200 °C; thermal loss, 0.5% of thermal input
Gas turbine	Discharge pressure, 1.047 bar; turbine polytrophic efficiency, 85%; mechanical/generator efficiency, 99%/99%
HRSG	Approach point ΔT, 10 °C; pinch point ΔT, 8 °C; thermal loss, 0.5% of thermal input
CO_2 compression	Single-stage compression ratio of CO_2 compressor, 3.5; compressor stage isentropic efficiency, 85%; cooling water inlet temperature, 15 °C; temperature at intercooler outlet, 30 °C; mechanical/electric efficiency, 99%/99%; liquid CO_2 to disposal, 30 °C and 121 bar
Balance of plant	Pump efficiency, 75%

Table 2. Approximate and elemental analyses of Illinois 6# coal

Proximate analysis (wt%)				Ultimate analysis (wt%)					
M_{ar}	A_{ar}	V_{ar}	FC_{ar}	C_d	H_d	O_d	N_d	$S_{t,d}$	A_d
10.00	8.91	32.22	48.87	69.62	5.33	10.03	1.25	3.87	9.90

the raw fuel gas leaves the gasifier at 1,371 °C with the pressure of 4.24 MPa. The gasifier oxidant feed was fixed at a value of 95% purity ($98\%O_2+1.5\%N_2+0.5\%Ar$). The reaction temperature and heat loss in the gasifier, which is assumed to be 1% of the total low heating value of the inlet coal flow, in the gasification reactor is maintained by adjusting the inlet flow rate of oxygen. In the simulation process, the carbon conversion rate is set to be 99%, and the mass flow of H_2O to coal is set to be 0.3 in the coal direct CLC process.

An activated amine solution (MDEA) is used to remove H_2S selectively with partial absorption of CO_2. The H_2S and COS removal efficiency are set to be 98.5%. Simultaneously, about 25% CO_2 is absorbed in this process. The purified gas component is shown in Table 2.

2. CLC Reactors

The proper oxygen carrier is the basis of successful operation of CLC. Ni-based oxygen carriers have been widely studied and results found that, $NiO/NiAl_2O_4$ had high reactivity with the mass ratio of NiO to $NiAl_2O_4$ equaled to 3 : 2 [7]. We selected $NiO/NiAl_2O_4$ (60 wt% : 40 wt%) as the oxygen carrier. Although the Ni-based oxygen carriers have high reactivity and stability [28-30], to maintain the reactivity and prevent the formation of the NO_x, the temperature of the AR was set under 1,200 °C. The reaction temperature affects the redox reaction rates, but given the high operating temperature and adequate residence time, in this simulation, it is assumed that all the reactions in those two CLC processes will reach their equilibria. This assumption is reasonable as the experimental results in continuous operation processes showed that the Ni-based oxygen carrier had high reactivity and the conversion of the combustible gases, such as H_2 and CO, could reach equilibrium [31-33]. Note that the CLC reactors are in the external interconnected circulating fluidized bed mode in the simulation process.

Two important design criteria for CLC are the circulation rate and the solids inventory of oxygen carrier particles between the air and fuel reactors [9]. In the CLC process, the circulation rate of the oxygen carrier between the reactors must be high enough to transfer the oxygen necessary for the fuel combustion and the heat necessary to maintain the heat balance [3]. Therefore, the circulation rate of the oxygen carrier should be determined by oxygen and heat balance in the system. The entraining gas flow will increase with the increase of the oxygen carrier circulation rate. Larger flows of the entraining gases and oxygen carrier particles increase the operation difficulties and increase the costs if they are outside the range of normal commercial experience. A lower circulation ratio between the two reactors not only can decrease the cost of the operation, but also can maintain the reactor at a reasonable reactor size. Here, the circulation ratio of the oxygen carrier, denoted by R, is defined as follows:

$$R=m_{OC}/m_{coal} \quad (9)$$

where the m_{OC} is the circulation rate of the oxygen carrier particles between the air and fuel reactors, kg/s; m_{coal} is the mass flow rate of the solid fuel introduced in the system, kg/s.

The solids inventory needed in the fuel reactor is determined by the oxygen carrier circulation rate and the residence time needed to convert the fuel. The residence time is related to the reactivity of the fuel and oxygen carrier particles. The particle size of the particles has a great effect on the reactivity oxygen carrier. Investigations on the Ni-based oxygen carriers found that a higher reaction rate could be obtained with a smaller particle size [34,35]. Higher reaction rates are most likely due to more surface area for the better gas-solid interaction, which can reduce the solids inventory in the system. Thus, a low reactivity in combination with high circu-

lation of oxygen carrier will mean a large solid inventory and thus large reactor sizes. The particle size of the oxygen carrier affects the overall reaction rate, and therefore affects the solids inventory and reactor size. However, the particles are easier to be elutriated if the particle size is too small, making the mass loss of the oxygen carriers. Therefore, the oxygen carrier particle size should be determined considering the reaction rate and the separation efficiency. Further examination needs to be conducted.

3. Gas Turbine

The gas turbine is the main work output device in the system. Because increasing the turbine inlet temperature (TIT) can raise the system efficiency, supplementary firing is used to increase the depleted air temperature of GT1. Since the volume of the flue gas from FR is relatively small, supplementary firing is not used for GT2. The supplementary firing rate is defined as follows:

$$\eta_b = M_{gb}/M_{gt} \quad (10)$$

where M_{gb} is the mass flow of the syngas for supplementary firing, and M_{gt} is the total mass flow of the syngas produced.

With the increase of the TIT, extra air will be used to cool the gas turbine; the definition of the cooling air ratio η_C is

$$\eta_C = M_C/M_A \quad (11)$$

where M_c is the mass flow of the cooling air, and M_A is the mass flow of the air at the inlet of the compressor.

There might be unreacted CO and H_2 in the flue gas of the FR; the incomplete conversion of the fuel will decrease the system efficiency and increase the work consumption of the CO_2 compressor. But the molar fraction of CO and H_2 is very low in the flue gas. The ultra-low concentration of combustible gases (CO and H_2) and relatively low temperature make it difficult to utilize with regular technologies. Catalytic combustion can achieve effective combustion at much lower temperatures than in conventional flame combustion, thus allowing for the simultaneous ultra-low emissions of NOx [36]. Here, catalytic combustion is used to convert the incomplete gases with pure oxygen.

4. Heat Recovery Steam Generator (HRSG) Device

In the coal gasification CLC system, an F-class gas turbine (pressure ratio 17, TIT 1,350 °C) is used as the model. Most of the reactions occur at high temperatures, resulting in a number of high temperature streams. The HRSG unit recovers the heat from the gaseous product streams, producing both high pressure and low pressure steams. A three-pressure reheat steam-water system is employed in the simulation process with the parameters of HP steam 12.5 MPa/565 °C, reheating steam 2.86 MPa/565 °C, and low pressure (LP) steam 0.72 MPa/232 °C. In the CDCL process, supplementary firing is not used for the flue gas from AR. Considering the lower temperature of the gas, PG6561B turbine (pressure ratio 12, TIT 1,104 °C) produced by GE company is used in the model. The parameters of steam-water system are the same with that in coal gasification CLC process.

In HRSG devices, assumptions are pinch point 8 °C, approach point 10 °C, back pressure in condenser 3.6 kPa, HPST isotropic efficiency 88%, IPST isotropic efficiency 92% and LPST isotropic efficiency 90%. In the coal gasification CLC system, the raw syngas from the gasifier is desulfurized, so the exhaust gas temperatures from AR and FR after HRSG are both cooled to 80 °C, while in the coal direct CLC system, the exhaust gas temperatures from AR and FR after HRSG are cooled to 80 °C and 130 °C, respectively.

5. CO_2 Separation and Compressor

The CO_2-rich stream is compressed in stages and cooled by circulating water. Meanwhile, condensate is removed. CO_2 is compressed to 121 bar in four intercooled stages. The inlet temperature of the circulating water is 15 °C. To measure the CO_2 capture performance of a system, the CO_2 capture efficiency is defined as follows:

$$\eta_{CO_2} = M_{CC}/M_{CT} \quad (12)$$

where η_{CO_2} is CO_2 capture efficiency; M_{CC} is CO_2 flow from FR after steam vapor condensing; M_{CT} is the total CO_2 flow of the plant.

Note that the utilization of the large quantity of CO_2 captured is a tough issue. It can be used in commercial chemical processes, but the large-scale applications are limited. Another way is to store the CO_2 captured in geological formations and the deep ocean, but the long-term performance of CO_2 in those reservoirs needs further study, especially the safety and the environmental effects [37]. The specific utilization method is out of the investigation scheme of this study.

RESULTS AND DISCUSSION

1. The Circulation Ratio of the Oxygen Carrier

1-1. Coal Gasification Chemical Looping Combustion Process

The molar fraction of the gases and solids from the FR with the value of R in the coal gasification CLC process is shown in Fig. 3. When R is larger than 8.675, the molar fraction of the gases does not change. As the gases mainly introduced are H_2 and CO, the reactions in the fuel reactor between the oxygen carrier and reducing gases are exothermic. Moreover, the oxygen carrier materials will also transport heat to the FR. Thus, the FR is exothermic in the coal gasification CLC process. This indicates that if the supply of the oxygen carrier can meet the oxygen balance of the reactor, the heat supply can be out of consideration. In the FR, the reactor is exothermic, the excess heat should be recovered to maintain the suitable operating temperature. One method is to lay the water wall to

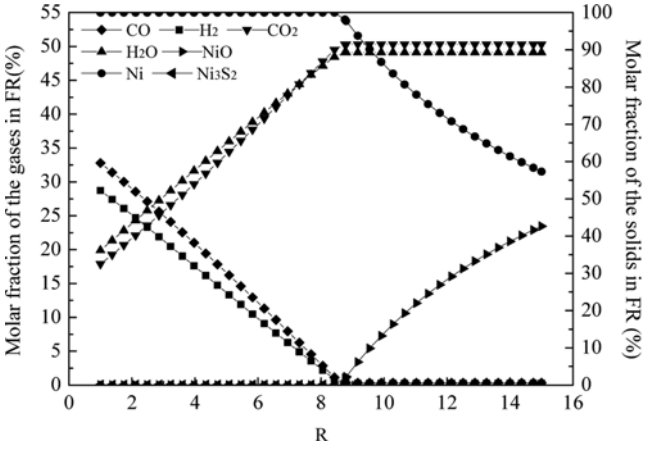

Fig. 3. The gas and solid composition from FR as a function of R.

generate high pressure steam for power generation. Another method is to introduce part of CO_2 to the FR. Considering the potential erosion of the boiler tubes by the oxygen carriers, the second method was adopted in this simulation processes.

When the value of R is set to be 8.675, the oxygen carrier can meet the heat and oxygen balance of the reactor. However, some of oxygen carrier particles will be lost due to fragmentation/attrition and their reaction activity maybe reduced for long time running, and thus part of oxygen carrier particles may have to be frequently supplemented and replaced. Moreover, in this paper, all the reactions in the CLC process are supposed to reach their equilibria. The circulation ratio of the oxygen carrier in coal gasification CLC process is determined by the stoichiometric oxygen balance, but gaseous fuels might suffer from the insufficient contact with the oxygen carrier. A part of gaseous fuels will be carried away from the FR without joining the reactions with the oxygen carrier. Therefore, in the real industrial process, the amount of the oxygen carrier should be larger than that calculated by oxygen balance. To maintain stable operation and ensure the full conversion of the fuels, ~10% excess oxygen carrier particles are added in the coal gasification CLC process during the simulation.

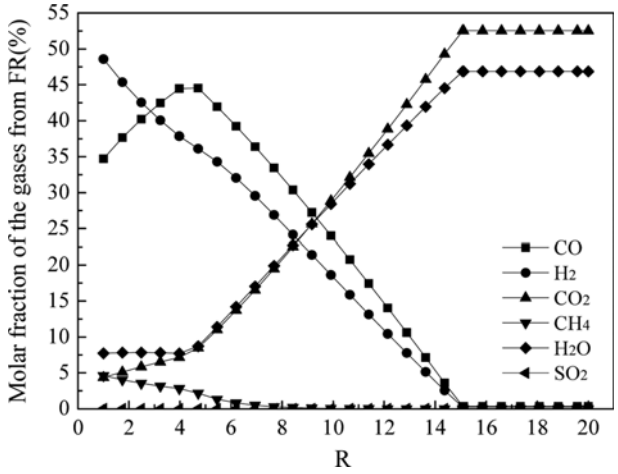

Fig. 4. The gas composition from FR as a function of R.

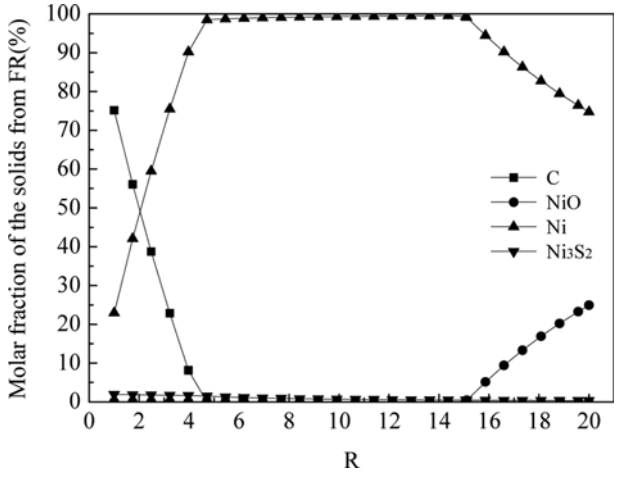

Fig. 5. The solid composition from FR as a function of R.

1-2. Coal Direct Chemical Looping Process

Assuming the temperature of the FR is 900 °C and AR 1,200 °C, Fig. 4 and Fig. 5 show the molar fraction of the gases and solids from the FR as a function of R in the direct coal CLC process. With the increase of the R, the conversion of coal goes up. When R is larger than 4.38, there is no C in the FR, while the molar fraction of the gases and solids does not change when R is larger than 15. The gases from the outlet of the FR are mainly CO_2 and H_2O, only with little fraction of CO and H_2. The appearance of incompletely converted CO and H_2 is due to the thermodynamic limits of Ni-based oxygen carriers [38]. As mentioned before, these small amounts of combustible gases can be converted by catalytic combustion using pure oxygen.

The concentration of CO increases with R, and then decreases. Because the mass flow rate of H_2O/coal in FR is 0.3, part of coal char is not gasified. When the amount of NiO increased, NiO would react with H_2 and CO according to reactions (6) and (7), following which the produced H_2O and CO_2 reacted with the coal char in the FR according to reactions (3) and (2). Therefore reactions (6) and (7) promote reaction (3), thus resulting in higher concentrations of CO. However, with the increase of R, syngas generated would react with NiO, and reactions (6) and (7) become the primary reactions, so the CO concentration goes down. Note that the curves of H_2 and CO concentrations are different, which reflects that H_2 is more reactive with NiO than that of CO.

Very small amount of SO_2 was observed. This is because the sulfur-containing species from the coal may be oxidized to SO_2 by oxidants such as H_2O, CO_2 or NiO. It also can be found that Ni_3S_2 will appear when the oxygen carrier is not enough. This is in accordance with the results obtained by other researchers. Jerndal et al. [39] found that Ni_3S_2 is the phase which is most likely to form at SO_2 and H_2S partial pressures and temperatures which may be encountered in a CLC fuel reactor. Wang et al. [40] studied the effect of oxygen excess number on the sulfur deposition and found that more sulfur deposition might form at oxygen-deficient conditions. The formation of Ni_3S_2 on the oxygen carrier particles could result in deactivation of the particles, and the relatively low melting points (789 °C) may deteriorate the operation performance of the parti-

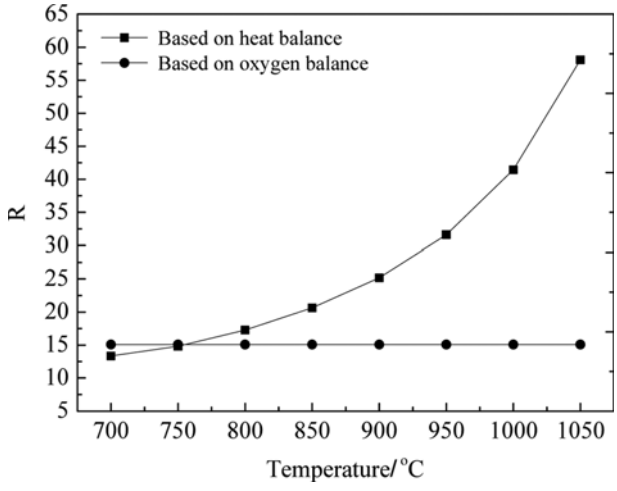

Fig. 6. The values of R as a function of FR temperature.

cles, which needs to be considered in the operation process.

To convert the fuels to the maximum degree, the value of R based on the oxygen demand can be determined by the method mentioned above. However, the circulation rate of oxygen carrier particles between the AR and FR should be determined both by oxygen and heat amount needed in the system. Thus, the ASPEN Plus model was used to calculate the circulation rate of the oxygen carrier based on heat balance at the given parameters of specified FR temperature and the corresponding heat loss.

The molar values of R as a function of FR temperature based on oxygen and heat balance, respectively, are shown in Fig. 6. The value of R based on oxygen balance does not change significantly with the increase of the FR temperature, while the value based on heat balance increase significantly. Note that, the reactions in the system are assumed to achieve thermodynamic equilibrium, so the value of R based on oxygen balance does not change greatly. However, the value of R based on heat balance increases from 13.34 to 41.42 when the temperature of the FR increases from 700 °C to 1,000 °C. This is because the temperature difference is smaller when the FR temperature increases. The circulation ratio of the oxygen carrier needs to be increased to supply enough oxygen carrier to maintain the temperature of the FR. It can be concluded that if the circulation ratio of the oxygen carrier can meet the heat balance of the reactor, the oxygen supply can also be met when the temperature of FR is higher than 750 °C. Therefore, the value of R should be determined by the heat balance in direct coal CLC process when using $Ni/NiAl_2O_4$ as an oxygen carrier. It can be found that the circulation ratio of the oxygen carrier obtained based on heat balance is larger than that based on oxygen balance. However, to maintain the high temperature of FR, the oxygen carrier circulation ratio should be set by the heat balance, and therefore, there will be a large amount of oxygen carrier that does not participate in the reaction, but only acts as the heat transfer medium in direct coal CLC process.

It can be concluded that the circulation rate of the oxygen carrier in coal gasification CLC process is much lower than that in coal direct CLC process. This can be explained by the complicated reactions in the FR of the coal direct CLC process. In the FR, the coal pyrolysis and gasification reactions happen. Simultaneously, the oxygen carrier is reduced by pyrolysis and gasification products. Although the heat of the reactions between the gases and the oxygen carrier highly depend on the type of oxygen carrier used, the total reactions in the fuel reactor are strongly endothermic, especially due to the highly endothermic pyrolysis and gasification reactions. Moreover, the vaporization of the steam also needs a heat supply. Therefore, more heat must be provided to drive the reactions. In the external interconnected circulating fluidized bed mode, the heat is supplied by the oxygen carrier from the air reactor, so the value of R is larger. In the coal gasification CLC process, however, only the reactions between the gases and the oxygen carrier happen. The heat consumed during the pyrolysis and gasification reactions is supplied by the combustion of part of fuel in the gasifier. In the CLC process, the temperature of FR is usually in the range of 750 °C and 1,000 °C. In this temperature range, a large part of the oxygen carrier only transfers heat as a heat transfer medium, but does not participate in the reaction in the direct coal CLC process, while in the coal gasification CLC process, the oxygen carrier not only acts as a heat transfer medium, but also is involves in the reaction.

In the coal direct CLC process, the circulation rate of the oxygen carrier between air and fuel reactors is very large to maintain the high temperature of FR. This will increase the operation cost and power consumption. A proper reactor design is also necessary for the efficient operation of the CLC process [41]. Son et al. [42] designed an annular shape circulating fluidized bed for CLC of methane. In the facility, the AR is surrounded by the FR; therefore, in this experimental apparatus the heat of the fuel reactor can be obtained in two ways, that is, the heat conducted from the air reactor and the heat transferred by the oxygen carrier particles. The circulation rate of the particles can be considerably smaller. This mode should be considered in the solid fuel CLC process.

2. The System Efficiency of Two Combined Cycles

To compare the two systems more intuitively, the values of system efficiency are shown in Fig. 7, assuming that the temperature of AR and FR is 1,200 °C and 900 °C, respectively. The system efficiency of direct coal CLC process can reach to 49.59% (LHV) with the CO_2 capture efficiency of almost 100%. Thus, this process can reach almost zero carbon emission. When the TIT is set at 1,350 °C, the cooling air ratio of 18%, the system efficiency of coal gasification CLC process can reach to 40.53% (LHV) with the CO_2 capture efficiency of 85.2%. It can be concluded that the system efficiency of the coal direct CLC process is higher than that of coal gasification CLC process. This may be due to the reasons as follows: First, pure oxygen is needed in the gasification process. The detailed power output and input of each unit in the system is shown

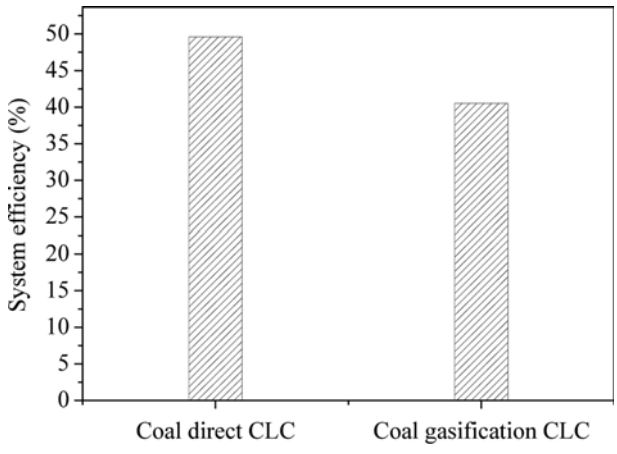

Fig. 7. The system efficiency of two combined cycles for CLC with coal.

Table 3. The purified gas component (vol%)

H_2O	N_2	Ar	H_2	CO	CO_2	H_2S	COS	NH_3
19.750	0.809	0.131	28.420	43.634	7.184	0.021	0.048	0.002

Table 4. Power balance over the two CLC combined cycles

Two combined cycles	Input						Output			Net power (MW)
	Air compressor	CO_2 compressor	Oxygen production	Oxygen compressor	HRSG bump	Slurry bump	Steam urbine	Gas turbine 1	Gas turbine 2	
Coal direct CLC	327.974	10.557	0.809	0.201	2.570	/	−238.081	−559.992	/	−495.962
Coal gasification CLC	272.921	50.598	46.645	17.644	2.278	0.104	−209.142	−471.150	−115.192	−405.294

Table 5. Power balance over the coal gasified CLC combined cycle at different AR temperatures

Temperature (°C)	Input						Output			Net power (MW)
	Air compressor	CO_2 compressor	Oxygen production	Oxygen compressor	HRSG bump	Slurry bump	Steam turbine	Gas turbine 1	Gas turbine 2	
950	300.719	17.121	46.118	17.507	2.292	0.104	−210.408	−553.261	−44.298	−424.106
1000	295.495	23.827	46.226	17.535	2.256	0.104	−207.141	−536.979	−58.591	−417.268
1050	289.643	30.863	46.348	17.567	2.262	0.104	−207.651	−519.748	−73.484	−414.096
1100	284.667	37.136	46.432	17.589	2.267	0.104	−208.105	−504.458	−86.833	−411.201
1150	278.852	43.915	46.536	17.616	2.272	0.104	−208.632	−487.755	−101.124	−408.216
1200	272.921	50.598	46.645	17.644	2.278	0.104	−209.142	−471.150	−115.192	−405.294

in Table 4. Note that the oxygen production process reduces the efficiency by about 4.66% in the coal gasification CLC combined cycle, while this value is only 0.81% in the coal direct CLC combined cycle. Therefore, the oxygen production will dramatically reduce the system efficiency. Second, the gasifier pressure is very high, while the FR pressure is limited by the gas turbine. Thus there is a significant pressure difference between the Texaco gasifier and the FR. It is needed to reduce the pressure of the gases before they are introduced into FR, which reduces the work capacity of the gases. Third, the complicated system of the coal gasification CLC will have more heat loss, especially in the radiant and convective heat exchangers.

Although the coal direct CLC process has higher system efficiency and higher CO_2 capture efficiency, there are many challenges associated with this technology. A slow conversion and conversion rate of the solid fuel has been observed [43], so a way to convert the solid fuel more efficiently should be studied [44,45]. The oxygen carriers with high stable reactivity, high attrition resistance, and low reactivity with ash and other contaminants are also a key aspect for the successful operation of CLC process. Moreover, the fuel ash may significantly reduce the lifetime of the oxygen carrier, so the separation between oxygen carrier and ash is a key issue [46]. Although the fuel ash could be separated from the oxygen carrier particles by the difference of density, there may be potential interactions between the oxygen carrier and solid fuel ash. Other challenges also include the design of a suitable reactor system to obtain an efficient process. However, those problems are not considered in this simulation process, as the reactions in the system are assumed to achieve thermodynamic equilibrium, and the separation of oxygen carrier from the unreacted fuel and ash is ideal.

Note that the coal gasification CLC process can change the system efficiency and CO_2 capture efficiency by adjusting the operation parameters, such as the AR temperature and the supplementary firing rate. The following two parts will discuss the effect of those two parameters on the system performance.

3. Effect of AR Temperature

The effects of AR temperature on the supplementary firing rate, system efficiency, and CO_2 capture efficiency are shown in Fig. 7, assuming that supplementary firing TIT is kept at 1,350 °C. The system efficiency will decrease with the increase of the AR temperature. When the AR temperature decreases from 1,200 °C to 950 °C, the system efficiency increases from 40.5% to 42.4%, while the CO_2 capture efficiency decreases from 85.2% to 54.9%, and also the corresponding supplementary firing rate decreases from 15.2% to 45.3%. When AR temperature increases, the flue of combustible gas bumped into the supplementary firing apparatus will decrease and therefore reduce the power output of GT1. Simultaneously, more combustible fuel gas is introduced into FR and the TIT of GT2 will increase, resulting in a higher power output. The power output and input of each unit in the system is shown in Table 5. The increase of AR temperature results in a lower total power output of the system.

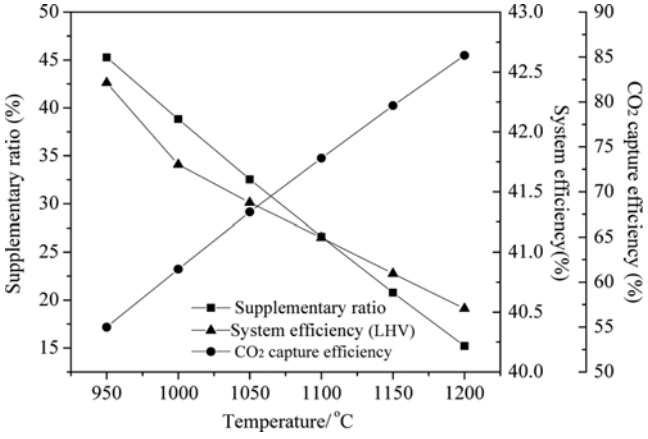

Fig. 8. The influence of the AR temperature on the supplementary ratio, system efficiency, and CO_2 capture efficiency.

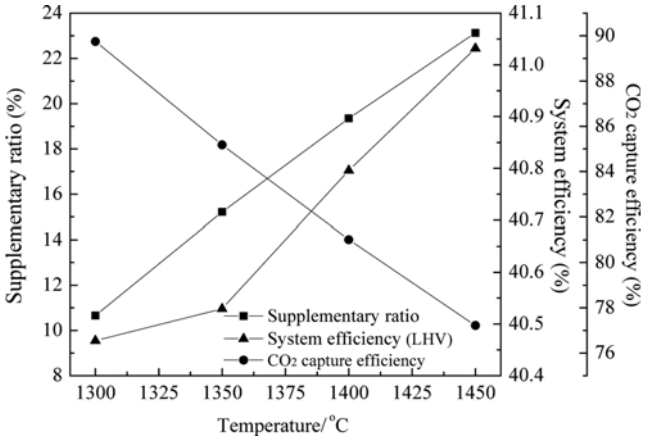

Fig. 9. The influence of the supplementary temperature on the supplementary ratio, system efficiency, and CO_2 capture efficiency.

4. Effect of Turbine Inlet Temperature (TIT)

The temperature at the AR outlet is only 1,200 °C in this study, which is relatively lower than F-class gas turbine TIT. Because increasing TIT can raise the plant electricity efficiency, supplementary firing is used to increase the temperature of the oxygen-depleted air. Four different TIT values (1,300 °C, 1,350 °C, 1,400 °C and 1,450 °C) are simulated with the cooling air fraction of 12%, 18%, 19%, and 20%. The fuel gas flow used for supplementary firing increases with the increase of supplementary firing TIT, which increases the gas turbine power output, whereas the fuel gas flow to FR goes down, which decreases the CO_2 expander power output. The plant power goes up because of the higher increase in gas turbine power.

As seen from Fig. 9, the system efficiency reaches 41.03% at 1,450 °C, whereas the CO_2 capture efficiency decreases from 89.75% to 77.22% with the TIT temperature increase from 1,300 °C to 1,450 °C. Therefore, in the coal gasification CLC system, the system efficiency can increase by supplementary firing, but at the expense of reducing the CO_2 capture efficiency.

CONCLUSION

Coal direct chemical-looping combustion (CLC) and coal gasification CLC processes are the two basic approaches to the application of the CLC technology with coal. The performance of two different CLC combined cycles with $NiO/NiAl_2O_4$ as an oxygen carrier was simulated and compared, which has been seldom investigated.

The oxygen carrier circulation ratio in two CLC process was calculated. The circulation ratio of the oxygen carrier in the coal gasification CLC process is smaller than that in the coal direct CLC process. When the temperature of the fuel reactor is in the range of 750-1,000 °C, the oxygen carrier in the coal gasification CLC transports both heat and oxygen, while a part of the oxygen carrier in the coal direct CLC process is only used as heat transfer medium but not reactant in the process.

The influence of the CLC process parameters on the system performance such as air reactor temperature and the turbine inlet supplementary firing temperature was investigated. In the coal direct CLC combined system, the system efficiency is 49.59% with the CO_2 capture efficiency of almost 100%, assuming the AR temperature at 1,200 °C and the FR temperature at 900 °C. As a comparison, the system efficiency of coal gasification CLC combined system is 40.53% with the CO_2 capture efficiency of 85.2% when the turbine inlet temperature is at 1,350 °C. Increasing the supplementary firing rate or decreasing the air reactor temperature can increase the system efficiency, but these will reduce the CO_2 capture efficiency.

ACKNOWLEDGEMENTS

This work was supported by the National Science and Technology Supporting Program of China (2011BAK06B04) and the Program for New Century Excellent Talents in University of Chinese Education Ministry (NCET-07-0678).

REFERENCES

1. Earth System Research Laboratory (ESRL), National Oceanic and Atmospheric Administration (NOAA), *Trends in atmospheric carbon dioxide*, http://www.esrl.noaa.gov/gmd/ccgg/trends/ (accessed April 1, 2014).
2. R. H. Socolow, *Sci. Am.*, **293**, 49 (2005).
3. A. Lyngfelt, B. Leckner and T. Mattisson, *Chem. Eng. Sci.*, **56**, 3101 (2001).
4. S. M. Benson and T. Surles, *Proc. IEEE*, **94**, 1795 (2006).
5. K. T. and John Davison, *Proceedings of the 7th International Conference on Greenhouse Gas Control Technologies*, Vancouver, Canada (2004).
6. R. Steeneveldt, B. Berger and T. A. Torp, *Chem. Eng. Res. Des.*, **84**, 739 (2006).
7. J. Adanez, A. Abad, F. Garcia-Labiano, P. Gayan and L. F. de Diego, *Prog. Energy Combust.*, **38**, 215 (2012).
8. H. Leion, T. Mattisson and A. Lyngfelt, *Fuel*, **86**, 1947 (2007).
9. T. Mattisson, A. Lyngfelt and H. Leion, *Int. J. Greenh. Gas Control*, **3**, 11 (2009).
10. H. Leion, T. Mattisson and A. Lyngfelt, *Int. J. Greenh. Gas Control*, **2**, 180 (2008).
11. S. A. Scott, J. S. Dennis, A. N. Hayhurst and T. Brown, *AIChE J.*, **52**, 3325 (2006).
12. A. Abad, T. Mattisson, A. Lyngfelt and M. Johansson, *Fuel*, **86**, 1021 (2007).
13. A. Abad, F. Garcia-Labiano, L. F. de Diego, P. Gayan and J. Adanez, *Energy Fuels*, **21**, 1843 (2007).
14. T. Mattisson, H. Leion and A. Lyngfelt, *Fuel*, **88**, 683 (2009).
15. H. Leion, T. Mattisson and A. Lyngfelt, *Energy Procedia*, **1**, 447 (2009).
16. A. Shulman, E. Cleverstam, T. Mattisson and A. Lyngfelt, *Fuel*, **90**, 941 (2011).
17. M. Ryden, A. Lyngfelt and T. Mattisson, *Int. J. Greenh. Gas Control*, **5**, 356 (2011).
18. M. Ryden, A. Lyngfelt and T. Mattisson, *10th International Conference on Greenhouse Gas Control Technologies*, Elsevier Science Bv, Amsterdam, 341 (2011).
19. G. Azimi, H. Leion, T. Mattisson and A. Lyngfelt, *10th Interna-*

tional Conference on Greenhouse Gas Control Technologies, Elsevier Science Bv, Amsterdam, 370 (2011).
20. M. Anheden and G. Svedberg, *Energy Convers. Manage.*, **39**, 1967 (1998).
21. O. Brandvoll and O. Bolland, *J. Eng. Gas Turb Power*, **126**, 316 (2004).
22. K. Marx, J. Bolhàr-Nordenkampf, T. Pröll and H. Hofbauer, *Int. J. Greenh. Gas Control*, **5**, 1199 (2011).
23. W. Xiang, S. Wang and T. Di, *Energy Fuels*, **22**, 961 (2008).
24. W. G. Xiang, S. Y. Chen, Z. P. Xue and X. Y. Sun, *Int. J. Hydrog. Energy*, **35**, 8580 (2010).
25. N. V. Gnanapragasam, B. V. Reddy and M. A. Rosen, *Int. J. Hydrog. Energy*, **34**, 2606 (2009).
26. F. X. Li, L. A. Zeng and L. S. Fan, *Fuel*, **89**, 3773 (2010).
27. A. J. Minchener, *Fuel*, **84**, 2222 (2005).
28. R. Kuusik, A. Trikkel, A. Lyngfelt and T. Mattisson, *Energy Procedia*, **1**, 3885 (2009).
29. K. S. Song, Y. S. Seo, H. K. Yoon and S. J. Cho, *Korean J. Chem. Eng.*, **20**, 471 (2003).
30. J.-I. Baek, C. Ryu, T. Eom, J. Lee, W.-S. Jeon and J. Yi, *Korean J. Chem. Eng.*, **28**, 2211 (2011).
31. E. Johansson, T. Mattisson, A. Lyngfelt and H. Thunman, *Chem. Eng. Res. Des.*, **84**, 819 (2006).
32. P. Kolbitsch, T. Proll, J. Bolhar-Nordenkampf and H. Hofbauer, *Int. J. Greenh. Gas Control*, **1**, 1465 (2009).
33. C. Dueso, F. Garcia-Labiano, J. Adanez, L. F. de Diego, P. Gayan and A. Abad, *Fuel*, **88**, 2357 (2009).
34. M. Ishida, H.G. Jin and T. Okamoto, *Energy Fuels*, **10**, 958 (1996).
35. R. Siriwardane, J. Poston, K. Chaudhari, A. Zinn, T. Simonyi and C. Robinson, *Energy Fuels*, **21**, 1582 (2007).
36. D. Trimm, *Appl. Catal.*, **7**, 249 (1983).
37. H. J. Herzog, *Environ. Sci. Technol.*, **35**, 148A (2001).
38. M. M. Hossain and H. I. de Lasa, *Chem. Eng. Sci.*, **63**, 4433 (2008).
39. E. Jerndal, T. Mattisson and A. Lyngfelt, *Chem. Eng. Res. Des.*, **84**, 795 (2006).
40. B. Wang, R. Yan, D. H. Lee, D. T. Liang, Y. Zheng, H. Zhao and C. Zheng, *Energy Fuels*, **22**, 1012 (2008).
41. H. J. Ryu, Y. C. Park, S. H. Jo and M. H. Park, *Korean J. Chem. Eng.*, **25**, 1178 (2008).
42. S. R. Son and S. D. Kim, *Ind. Eng. Chem. Res.*, **45**, 2689 (2006).
43. N. Berguerand and A. Lyngfelt, *Fuel*, **87**, 2713 (2008).
44. M. Luo, S. Wang, L. Wang, M. Lv, L. Qian and H. Fu, *Fuel Process. Technol.*, **110**, 258 (2013).
45. J. B. Yang, N. S. Cai and Z. S. Li, *Energy Fuels*, **22**, 2570 (2008).
46. Y. Cao and W. P. Pan, *Energy Fuels*, **20**, 1836 (2006).